Measurement of Spontaneous Transfer and Transbilayer Movement of BODIPY-Labeled Lipids in Lipid Vesicles†

Jining Bai‡,§ and Richard E. Pagano*,‡,||

Carnegie Institution of Washington, Baltimore, Maryland 21210, and Mayo Clinic and Foundation, Department of Biochemistry and Molecular Biology, 200 First Street, S.W., Rochester, Minnesota 55905

Received January 23, 1997; Revised Manuscript Received April 23, 1997⊗

ABSTRACT: An assay was developed to study the spontaneous transfer and transbilayer movement (flip−flop) of lipid analogs labeled with the fluorescent fatty acid, 5-(5,7-dimethyl BODIPY)-1-pentanoic acid (C_5-DMB-) in large unilamellar lipid vesicles comprised of 1-palmitoyl-2-oleoyl phosphatidylcholine (POPC). The assay is based on the concentration-dependent changes in fluorescence intensity that occur when donor vesicles containing a C_5-DMB-lipid are mixed with nonfluorescent acceptor vesicles. A kinetic model was developed to describe the time-dependent changes in concentration of a lipid undergoing both spontaneous transfer between unilamellar vesicles and transbilayer movement within the vesicle membranes, and a mathematical solution was obtained. Data were obtained using C_5-DMB-labeled analogs of sphingomyelin (C_5-DMB-SM), ceramide (C_5-DMB-Cer), phosphatidylcholine (C_5-DMB-PC), and diacylglycerol (C_5-DMB-DAG), and kinetic parameters for each lipid were determined using a nonlinear least-squares fitting program. The half-times for interbilayer transfer of the lipids were C_5-DMB-SM (21 s) < C_5-DMB-PC (350 s) ≈ C_5-DMB-Cer (400 s) ≪ C_5-DMB-DAG (100 h). C_5-DMB-Cer ($t_{1/2}$ ≈ 22 min) and C_5-DMB-DAG ($t_{1/2}$ ≈ 70 ms) exhibited rapid spontaneous transbilayer movement, while C_5-DMB-SM ($t_{1/2}$ ≈ 3.3 h) and C_5-DMB-PC ($t_{1/2}$ ≈ 7.5 h) moved across the bilayer very slowly. These results provide a basis for interpreting the behavior of these lipid analogs in cells.

Fluorescent lipid analogs have been useful for studying membrane lipid traffic in animal cells (reviewed in 1−3). In this approach, one of the naturally occurring fatty acids of a lipid is replaced with a short-chain fluorescent fatty acid, resulting in a fluorescent lipid analog that is more water soluble than its endogenous counterpart and that consequently can be readily integrated into cellular membranes by spontaneous lipid transfer from an exogenous source. The intracellular distribution of the labeled molecules can then be observed in living cells by high-resolution fluorescence microscopy, and temporal changes in the distribution of a given lipid (and its metabolites) can be correlated with changes in its metabolism. From such studies, it is possible to define the pathways of transport of a particular lipid analog and to study the underlying mechanism(s) of that transport. This approach has been particularly successful in studying lipid analogs labeled with *N*-(4-nitrobenzo-2-oxa-1,3-diazole)aminocaproic acid (C_6-NBD-). In the case of the C_6-NBD-labeled lipids, biophysical studies of the rates of spontaneous transfer of the lipid analogs between artificial membranes (*4*, *5*), as well as studies of their ability (or inability) to undergo transbilayer movement (flip−flop) in such systems (*6*−*8*), have provided important information for studying the mechanisms for intracellular transport of these analogs. For example, the finding that C_6-NBD-ceramide undergoes spontaneous flip−flop in model membranes and exhibits a high rate of spontaneous transfer *in vitro* (*7*), provides a rational explanation for the observation that this lipid labels intracellular membranes (e.g., the endoplasmic reticulum, nuclear envelope, and mitochondria) of living cells at low temperature. In contrast, the finding that other C_6-NBD-lipids, which exhibit rapid spontaneous transfer in liposomes but do not exhibit appreciable flip−flop in those systems, has led to the postulate of facilitated transbilayer movement of some of those lipids in cellular membranes (*9*−*13*).

Recently, we have begun to extend the approach noted above using lipids labeled with *N*-[5-(5,7-dimethyl-BODIPY)-1-pentanoic acid (C_5-DMB-) (*14*, *15a*). These analogs are a particularly attractive alternative to NBD-labeled lipids because the BODIPY fluorophore (i) has a higher fluorescence yield and is more photostable than NBD (*16*), and (ii) is less polar than NBD and therefore is probably better anchored in the membrane bilayer than NBD which loops back to the membrane−water interface (*17*, *18*). Futhermore, lipids labeled with C_5-DMB-fatty acids exhibit a shift in their fluorescence emission maximum from green to red wavelengths with increasing concentration in membranes (*14*). Thus, it is possible to distinguish membranes within the same cell that contain different concentrations of a fluorescent lipid and, using quantitative microscopy, to estimate the apparent concentration of the lipid in a particular organelle. This approach has been used to study the localization of C_5-DMB-Cer at the Golgi appartus of cultured cells (*14*) and the internalization and sorting of C_5-DMB-glucosylceramide (*15a*) and C_5-DMB-SM (*15b*) from the plasma membrane of human skin fibroblasts.

While C_5-DMB-lipids have a number of properties useful for cellular studies, to date, there are no biophysical studies of their rates of spontaneous transfer and flip−flop in

† Supported by USPHS Grant R37 GM-22942.

* Corresponding author. Tel: (507) 284-8754. Fax: (507) 284-4521. E-mail: pagano.richard@mayo.edu.

‡ Carnegie Institution of Washington.

§ Current address: Dept. of Pathology, Johns Hopkins School of Medicine, Baltimore, MD 21205.

|| Mayo Clinic and Foundation.

⊗ Abstract published in *Advance ACS Abstracts,* June 15, 1997.

S0006-2960(97)00145-1 CCC: $14.00

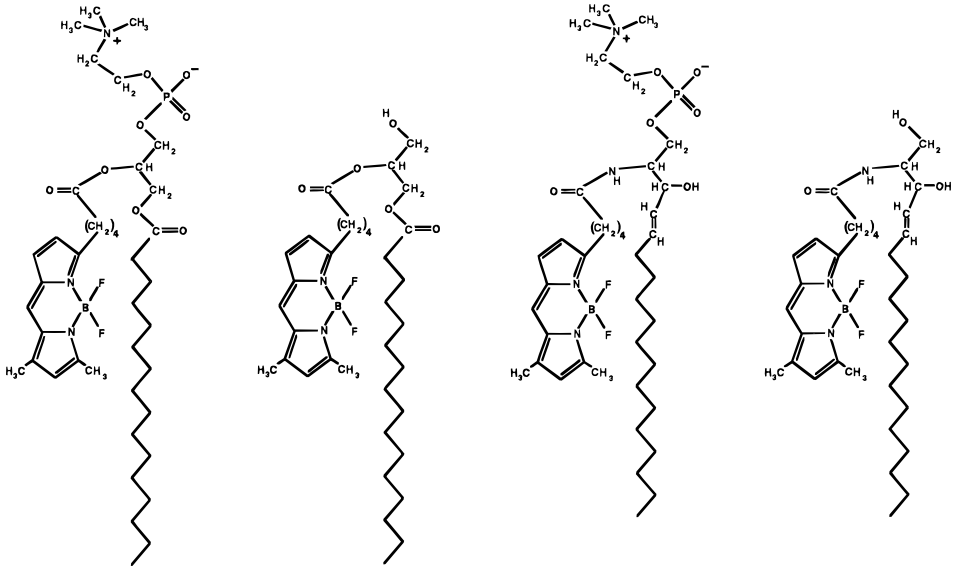

FIGURE 1: Structures of BODIPY-labeled lipids used in the present study. Phosphatidylcholine (PC), diacylglycerol (DAG), sphingomyelin (SM), and ceramide (Cer).

membranes. Thus, inferences about mechanisms of intracellular transport have to be made by analogy to the biophysical properties of other fluorescent lipid analogs. In the present study, a kinetic model was developed to describe the coupled processes of spontaneous lipid transfer and transbilayer movement of lipids and a mathematical solution was obtained. The time-dependent changes in the concentration of various C_5-DMB-lipid analogs (see Figure 1) were then determined by measuring changes in fluorescence intensity that occurred when donor and acceptor vesicles were mixed together, and the kinetic parameters for spontaneous transfer and flip−flop were determined by a nonlinear least-squares fitting program. While a number of publications pertaining to the kinetic modeling of these processes have appeared (*19*−*22*, *36*, *37*), the current study is unique in that it provides a more precise correlation with experimental observations when the spontaneous transfer and transbilayer movement of a given lipid are strongly coupled.

MATERIALS AND METHODS

Lipids. 1-palmitoyl-2-oleoyl phosphatidylcholine (POPC) was purchased from Avanti Biochemicals (Pelham, AL). *N*-[5-(5,7-dimethyl BODIPY)-1-pentanoyl]-D-*erythro*-sphingosine (C_5-DMB-Cer), -sphingosylphosphorylcholine (D-*erythro*-isomer) (C_5-DMB-SM), and 1,2 (palmitoyl-5,7-dimethyl BODIPY-1-pentanoyl)-phosphatidylcholine (C_5-DMB-PC) were obtained from Molecular Probes, Inc. (Eugene, OR). C_5-DMB-PC was hydrolyzed to the corrresponding fluorescent diacylglycerol (C_5-DMB-DAG) by digestion with phospholipase C (*23*) and purified by thin-layer chromatography. All lipids were stored in chloroform/methanol at −80 °C, periodically analyzed for purity by thin-layer chromatography, and repurified when necessary. The concentration of lipid stock solutions were determined by measurement of lipid phosphorus (*24*) or by reference to known concentrations of fluorescent standards.

Fluorescence Measurements. Fluorescence measurements were carried out in an SLM 8000C fluorimeter (Urbana, IL) using the "slow time course" mode. Samples were excited at 480 nm, and the fluorescence emission was detected at 510 nm at room temperature.

Preparation of Lipid Vesicles. Large unilamellar vesicles were prepared by extrusion (LUVETs) (*25*) and were approximately ∼1000 Å in diameter. Briefly POPC, with or without C_5-DMB-lipid, was dried under nitrogen, desiccated under vacuum, and then dispersed into 18 mM Hepes-buffered calcium- and magnesium-free Puck's saline, pH 7.4 (HCMF), using a vortex mixer to produce multilamellar vesicles. These vesicles were subjected to five cycles of freezing in liquid nitrogen and thawing at 40 °C. The vesicles were then extruded 10 times through two stacked polycarbonate filters (0.1 μm pore size) to produce large unilamellar vesicles.

Generation of Standard Curve. A standard curve was generated ($\lambda_{ex} = 480$ nm; $\lambda_{em} = 510$ nm) at room temperature by measuring the fluorescence intensities of LUVs comprised of POPC and containing various amounts of the C_5-DMB labeled lipids. The fluorescence intensity was then plotted *vs* mole fraction.

Kinetic Measurements and Calculations. In a typical experiment, an aliquot of acceptor vesicles was added to a cuvette containing an equal volume (1 mL) of fluorescent donor vesicles at time zero. The sample was stirred continuously, and all measurements were made at room temperature (22 °C). The concentration of donor vesicles was 15 μM POPC + 1.5 μM C_5-DMB-lipid; the acceptor vesicle concentration was either 120 or 240 μM POPC.

The changes in fluorescence intensities with time can be described by

$$F(t) = \mathrm{SC}([\mathrm{C}]^{\mathrm{D}}_{\mathrm{in}}) + \mathrm{SC}([\mathrm{C}]^{\mathrm{D}}_{\mathrm{out}}) + \mathrm{SC}([\mathrm{C}]^{\mathrm{A}}_{\mathrm{out}}) + \mathrm{SC}([\mathrm{C}]^{\mathrm{A}}_{\mathrm{in}})$$

where SC is the empirical function obtained from the standard curve, [C] represents the concentration of the fluorescent lipid in the outer (out) or inner (in) leaflet of the donor (D) or acceptor (A) membrane, and is defined by eq B4 in Appendix B.

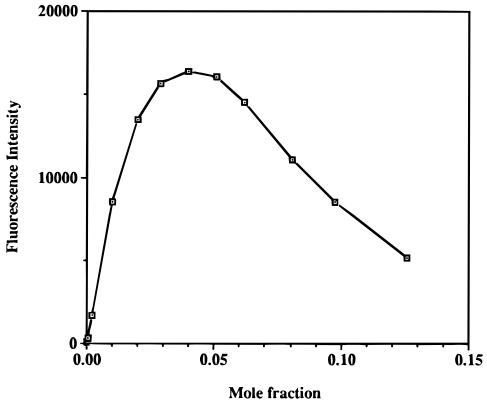

FIGURE 2: Standard curve of fluorescence intensity *vs* mole fraction for C_5-DMB-SM. The fluorescence intensity (λ_{ex} = 480 nm; λ_{em} = 510 nm) of large unilamellar vesicles formed from POPC and containing various amounts of C_5-DMB-SM was determined at room temperature. The POPC concentration was 15 μM for each data point. The shape of the standard curves between 0 and 12.5 mol % were similar for all four C_5-DMB-lipids studied.

Nonlinear Least-Squares Fitting. The data from the time course experiments were analyzed using the program NONLIN (*26a*,*b*) on the UNIX platform. Separate programs, which described the mathematical solutions of the coupled spontaneous transfer and transbilayer movement, the input−output information, and the empirical standard curves for each C_5-DMB-labeled lipid were compiled in FORTRAN 77 and used as entrance and exit connections for NONLIN.

RESULTS AND DISCUSSION

Standard Curves of C_5-DMB-Fluorescence vs Concentration. The standard curves for each fluorescent lipid were obtained at room temperature by measuring the fluorescence intensity (λ_{ex} = 480 nm; λ_{em} = 510 nm) for lipid vesicles containing various concentrations of the C_5-DMB-lipid. The shapes of the standard curve were similar for all four C_5-DMB-lipids used over the range of 0−12.5 mol %. Figure 2 shows a typical standard curve for C_5-DMB-SM. Between 0 and 2 mol %, the fluorescence intensity increased linearly. The fluorescence intensity reached a peak at 4 mol % and decreased steadily with increasing concentrations of the C_5-DMB-lipid, presumably because of self-quenching.

Time Course Measurements. Equal volumes of solutions containing various amounts of donor and acceptor vesicles were mixed at time zero, and the fluorescence intensity was then measured continuously. In each case, the resulting curves could be fitted by a double-exponential function (Appendix B). C_5-DMB-SM and -PC exhibited fast vesicle−vesicle transfer, which was characterized by a sharp linear increase in fluorescence intensity at early time points, a slower increase in fluorescence intensity at intermediate times, and a barely detectable change in the slope of intensity *vs* time after 30 min. This latter observation reflects a slow transmembrane movement. However, in the case of C_5-DMB-DAG, and -Cer, the increase in fluorescence intensity at early time points was moderate compared to C_5-DMB-SM and -PC and continued to increase with a considerable rate after hours, reflecting a strong coupling of the spontaneous transfer and flip−flop. The time to reach equilibrium varied significantly depending on the lipid species and ratio of donor to acceptor vesicles. In general, it increases in the order SM < PC < Cer < DAG. Figure 3 shows typical time course measurements for C_5-DMB-Cer and C_5-DMB-SM.

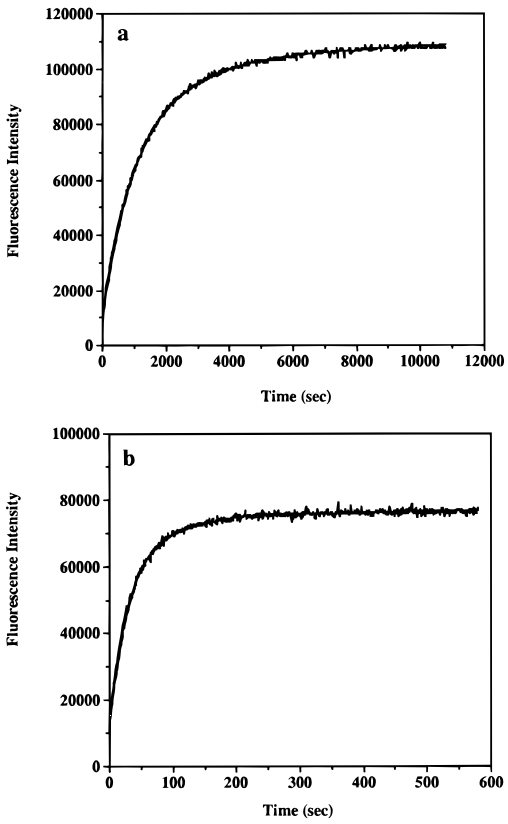

FIGURE 3: Spontaneous transfer of C_5-DMB-Cer between donor and acceptor vesicles. LUV donor vesicles (15 μM POPC) containing 10 mol % (a) C_5-DMB-Cer or (b) C_5-DMB-SM were mixed at time zero with a 16-fold excess of LUV acceptor vesicles formed from POPC. The sample was stirred continuously and the fluorescence intensity (λ_{ex} = 480 nm; λ_{em} = 510 nm) monitored over time at 22 °C. Dashed line, results of the NONLIN curve fitting program (see text for details); solid line, experimental data.

Table 1: Estimated Rate Values of Spontaneous Transfer[a]

lipid	A:D = *N*	K_+ (s^{-1})	K_- (s^{-1})	K_{m-} (s^{-1})
C_5-DMB-Cer	16	1.5×10^{-3}	9.2×10^{-5}	1.9×10^{-3}
	8	1.4×10^{-3}	1.8×10^{-4}	1.6×10^{-3}
C_5-DMB-DAG	16	2.1×10^{-5}	1.3×10^{-6}	2.2×10^{-5}
	8	1.8×10^{-5}	2.2×10^{-6}	2.0×10^{-5}
C_5-DMB-SM	16	3.2×10^{-2}	2.0×10^{-3}	3.4×10^{-2}
	8	3.9×10^{-2}	4.9×10^{-3}	3.9×10^{-2}
C_5-DMB-PC	16	2.1×10^{-3}	1.3×10^{-4}	2.2×10^{-3}
	8	2.0×10^{-3}	2.5×10^{-4}	2.0×10^{-3}

[a] *N* = ratio of acceptor (A) to donor (D) vesicles. K_{m-} = dissociation constant for monomeric transfer (see Figure 4). K_+ and K_- are defined in Figure 6.

The rate of spontaneous transfer can be estimated from the initial slope of the time course data combined with the information from the standard curve (eqs B5.1−B5.3). Table 1 shows the estimated rates for spontaneous transfer of each C_5-DMB-labeled lipid used in the presnt study.

Kinetic Parameters. All calculations were based on the equations derived in the Appendix (A4, B1−3). Subprograms were compiled in FORTRAN 77 in order to convey the information to NONLIN. The estimated rates were inputed into the NONLIN program as the starting point for the fitting calculations in order to generate accurate output results. The values of the rates for spontaneous transfer and transbilayer movement, as well as the relaxation times, are

Table 2: Kinetic Parameters of Spontaneous Transfer and Transbilayer Movement[a]

lipid	A:D = N	τ_2 (s)	τ_3 (s)	K_f (s^{-1})	K_{m-} (s^{-1})
C_5-DMB-Cer	16	$4.0 \times 10^{+2}$	$2.7 \times 10^{+3}$	5.0×10^{-4}	1.9×10^{-3}
	8	$4.1 \times 10^{+2}$	$2.6 \times 10^{+3}$	5.5×10^{-4}	1.7×10^{-3}
C_5-DMB-DAG	16	5.0×10^{-2}	$9.1 \times 10^{+4}$	$1.0 \times 10^{+1}$	2.2×10^{-5}
	8	5.0×10^{-2}	$1.2 \times 10^{+5}$	$1.1 \times 10^{+1}$	1.7×10^{-5}
C_5-DMB-SM	16	$3.2 \times 10^{+1}$	$1.8 \times 10^{+4}$	5.5×10^{-5}	3.1×10^{-2}
	8	$2.9 \times 10^{+1}$	$1.5 \times 10^{+4}$	6.9×10^{-5}	3.4×10^{-2}
C_5-DMB-PC	16	$4.9 \times 10^{+2}$	$4.6 \times 10^{+4}$	2.2×10^{-5}	2.0×10^{-3}
	8	$5.2 \times 10^{+2}$	$3.4 \times 10^{+4}$	3.0×10^{-5}	1.9×10^{-3}

[a] A, D, N, (s^{-1}), and K_{m-} are defined in the legend of Table 1. τ_2 and τ_3 = relaxation times defined by eqs A4.3 and A4.4. K_f = rate constant for transbilayer movement (refer to Figure 5).

Table 3: Half Times for Spontaneous Transfer and Transbilayer Movement

	C_5-DMB-Cer	C_5-DMB-DAG	C_5-DMB-SM	C_5-DMB-PC
$Tf_{1/2}$ (s)	$1.3 \times 10^{+3}$	7.0×10^{-2}	$1.2 \times 10^{+4}$	$2.7 \times 10^{+4}$
$Tex_{1/2}$ (s)	$4.0 \times 10^{+2}$	$3.6 \times 10^{+5}$	$2.1 \times 10^{+1}$	$3.5 \times 10^{+2}$

[a] $Tf_{1/2}$ (= ln $2/K_f$) and $Tex_{1/2}$ (= ln $2/K_{m-}$) correspond to the half-times for transbilayer movement (flip-flop) and spontaneous monomeric transfer, respectively, at 22 °C. Errors in estimation of the half-times were ≤10%. Values were obtained at 22 °C.

listed in Table 2. In general, the rates for spontaneous transfer increase in the order of DAG < Cer < PC < SM, whereas the rates for transbilayer movement increase in the order of PC < SM < Cer < DAG. The half-times for spontaneous transfer and transbilayer movement of each of the fluorescent lipids were calculated from the corresponding rate constants based on $t_{1/2} = (1/k)\ln 2$ and are listed in Table 3.

In the present study, we have examined C_5-DMB-PC *vs* C_5-DMB-DAG and C_5-DMB-SM *vs* C_5-DMB-Cer. Within each pair, the backbone of the different molecules is identical while the polar head groups are different (refer to Figure 1). On the basis of the data in Tables 2 and 3 for these lipids, we can make the following points.

(1) The half-times for spontaneous interbilayer transfer of C_5-DMB-lipids are significantly longer than those obtained using C_6-NBD-lipids. Several different methods have been used previously to quantify the half-times for spontaneous transfer of various NBD-labeled lipids in lipid vesicles (*21*, *22*). The rates of spontaneous transfer of the C_6-NBD-lipids are about an order of magnitude faster than for the corresponding C_5-DMB-lipids [e.g., $t_{1/2} \approx 25$ s for C_6-NBD-PC (*22*) *vs* 350 s for C_5-DMB-PC). While this difference might be due to differences in vesicle size (*34*) in the various experiments, it most likely reflects the fact that the DMB moiety is more hydrophobic than the NBD group and therefore is probably better anchored in the membrane bilayer. Indeed, it has been shown by two different methods that the NBD group loops back to the membrane−water interface (*17*, *18*). The difference in half-times is also reflected in cellular studies in which it has been found that C_6-NBD-lipids present in the outer leaflet of the plasma membrane can be readily back-exchanged from the cell surface by incubation with a non-fluorescent acceptor (e.g., lipid vesicles or BSA) (*9*, *12*, *27*, *28*), while removal of C_5-DMB-lipids from the plasma membrane is much more difficult, requiring long incubation times and high concentrations of acceptor (*14*, *15a*,*b*). Thus, while much useful information concerning intracellular transport of lipids has been obtained using C_6-NBD-lipids, it is important to extend this approach to more hydrophobic analogs such as the C_5-DMB-lipids, whose slower rates of spontaneous transfer make them more similar to natural lipids.

(2) Both the head group and backbone affect the rate of lipid flip−flop and spontaneous transfer. While it has previously been shown that the lipid head group plays an important role in these processes (*29*−*31*), we also show here that the lipid backbone influences this behavior. In general, the spontaneous transfer rates of sphingolipids are significantly greater than those of the glycerolipids with the same headgroup. This is particularly apparent when comparing the half-time for spontaneous transfer of the C_5-DMB-analogs of ceramide (400 s) *vs* diacylglycerol (100 h). The reason for this difference is unknown but may be related to the polarity or the flexibility of the lipid backbones.

(3) The flip−flop of C_5-DMB-PC is comparable to that of a nonfluorescent lipid. Previous reports have examined the transbilayer movement of PC (and PC analogs) in various systems, with values for the half-times varying widely from 9 h to >100 h at room temperature (*1*, *32*−*34*). The results for C_5-DMB-PC ($t_{1/2} \approx 7.5$ h) are similar to those obtained for dimyristoyl PC ($t_{1/2} \approx 9.6$ h) in LUV (*34*).

(4) The half-times for spontaneous transfer and flip−flop of C_5-DMB-Cer and -DAG suggest that endogenous Cer and DAG are transported differently within cells. Both DAG and Cer are thought to be generated at the plasma membrane of cells in response to appropriate extracellular signals, serving in turn as lipid second messengers. C_5-DMB-DAG exhibits a significant rate of flip−flop and a very small rate of spontaneous transfer, suggesting that endogenous DAG generated at the plasma membrane would initially be restricted to the plasma membrane. The fact that protein kinase C binds to the plasma membrane upon activation (*35*) is consistent with this idea. In contrast, C_5-DMB-Cer exhibits moderate rates for both flip−flop and spontaneous transfer, raising the possibility that endogenous Cer might be more readily accessible to other intracellular compartments once it is generated at a particular site.

ACKNOWLEDGMENT

The authors thank Dr. L. Brand (Biology Department, The Johns Hopkins University) for making the NONLIN program available to us and providing assistance, members of the Pagano Laboratory for helpful suggestions, and Dr. Zeljko Bajzer (Mayo Clinic and Foundation) for critically reading the manuscript.

APPENDIX A: KINETIC MODEL AND MATHEMATICAL SOLUTION FOR COUPLED SPONTANEOUS TRANSFER AND TRANSBILAYER MOVEMENT OF LIPIDS

The schematic in Figure 5 and the accompanying equations (A2) describe the coupled processes of spontaneous transfer and transbilayer movement of a lipid moving between (and across the bilayer of) lipid vesicles. This treatment is based on the model shown in Figure 4 and eq A1, which was developed by others (*19*−*22*, *30*, *31*, *36*, *37*). The current model can be treated as four, reversible reaction steps; however, the mathematical solution is extremely complex. A suitable solution for this model was first obtained by Arvinte and Hildenbrand (*36*) using the assumption that $K_f \ll K_-$, resulting in a set of three-exponential functions. In

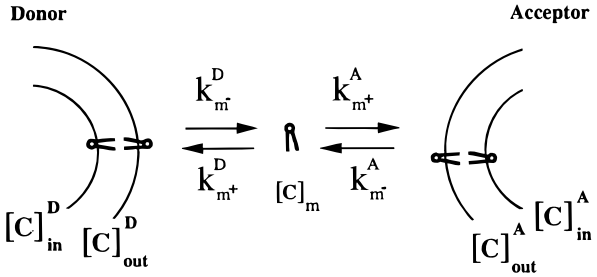

$$\frac{d[C]^D_{out}}{dt} = -k^D_{m-}[C]^D_{out} + k^D_{m+}[C]_m S^D \quad \text{(A1.1)}$$

$$\frac{d[C]^A_{out}}{dt} = -k^A_{m-}[C]^A_{out} + k^A_{m+}[C]_m S^A \quad \text{(A1.2)}$$

$$\frac{d[C]_{in}}{dt} = 0 \quad \text{(A1.3)}$$

The mathematical solution has been solved in ref 4.

FIGURE 4: Kinetic model for spontaneous transfer of lipids in lipid vesicles. k_m- and k_m+ represent respectively the off-rate and on-rate for monomer exchange. [C] represents the lipid concentration in a given compartment. The superscripts A and D represent the acceptor and donor vesicles, and the subscripts out and in represent the outer and inner leaflets of the membrane bilayer. k_m- and k_m+ represent the off-rate and on-rate for monomer exchange. S is the total surface area of the donor or acceptor vesicles and m represents the monomeric state. Refer to refs 19−22, 30, 31, 36, and 37.

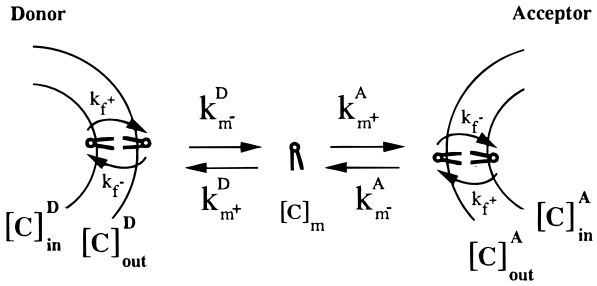

differential equation:

$$\frac{d[C]^D_{in}}{dt} = -k_{f+}[C]^D_{in} + k_{f-}[C]^D_{out} \quad \text{(A2.1)}$$

$$\frac{d[C]^D_{out}}{dt} = k_{f+}[C]^D_{in} - (k_{f-} + k^D_{m-})[C]^D_{out} + k^D_{m+}[C]_m S^D \quad \text{(A2.2)}$$

$$\frac{d[C]^A_{out}}{dt} = k_{f+}[C]^A_{in} - (k_{f-} + k^A_{m-})[C]^A_{out} + k^A_{m+}[C]_m S^A \quad \text{(A2.3)}$$

$$\frac{d[C]^A_{in}}{dt} = -k_{f+}[C]^A_{in} + k_{f-}[C]^A_{out} \quad \text{(A2.4)}$$

$$\frac{d[C]_m}{dt} = k^D_{m-}[C]^D_{out} + k^A_{m-}[C]^A_{out} - (k^D_{m+}S^D + k^A_{m+}S^A)[C]_m = 0 \quad \text{(A2.5)}$$

FIGURE 5: Kinetic model for the coupled processes of spontaneous transfer and transbilayer movement of lipids in lipid vesicles. The equations accompanying this schematic (A2.1−A2.5) are based on the model in Figure 4 and eqs A1.1−A1.3, and the work of others [*19*−*22*, *30*, *31*, *36*, *37*]. Setting eq A2.5 = 0 has been a common theme for all previous models. Since the rate-limiting step in spontaneous transfer of lipids is the dissociation of lipid monomers from the membrane into the aqueous phase, $[C]_m$ has been treated as steady state. K_f- and K_f+ represent the rate constants for transbilayer movement (flip-flop) outside to inside and inside to outside respectively; other terms are defined in the legend to Figure 4.

a later study, Storch and Kleinfied (*37*) used a numerical calculation program called MASYMA to solve eq A2, resulting in a set of four-exponential functions. On the other hand, the experimental observations of coupled spontaneous transfer and transbilayer movement have always shown double-exponential behavior (and change to single-exponential under certain extreme conditions) (*36*, *41*, *42*). As a result, the mathematical solutions noted above have not been extensively applied. Instead, most of the quantitative studies to date have been performed empirically (*34*, *36*, *38*−*41*) by assuming the process is a double-exponential function, $[A_1 \exp(B_1 t) + A_2 \exp(B_2 t)]$, and fitting the pre-exponential variables A_1 and A_2 and superexponential variables B_1 and B_2 independently. This empirical method avoids the requirement of a detailed mathematical solution for the coupled processes of spontaneous transfer and transbilayer movement. However, there are some negative aspects to this approach. (i) A_1 and A_2 are actually related to B_1 and B_2. (More uncertainty and flexibility could be introduced in the resulting kinetic parameters by treating A_1, A_2, B_1 and B_2 independently.) (ii) The fast and slow components must be arbitrarily assigned to each process (usually spontaneous transfer is assigned as "fast" and transbilayer movement as "slow"). However, in actuality, both spontaneous transfer and transbilayer movement can contribute to both the fast and slow components.

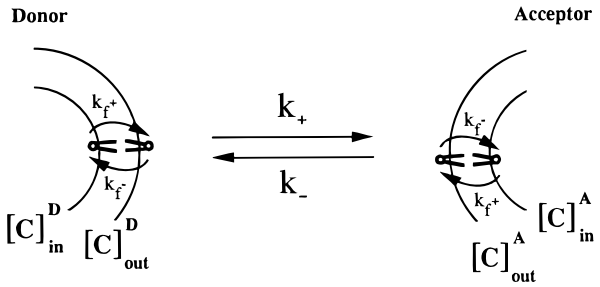

$$\frac{d[C]^D_{in}}{dt} = -k_{f+}[C]^D_{in} + k_{f-}[C]^D_{out} \quad \text{(A3.1)}$$

$$\frac{d[C]^D_{out}}{dt} = k_{f+}[C]^D_{in} - (k_{f-} + k_+)[C]^D_{out} + k_-[C]^A_{out} \quad \text{(A3.2)}$$

$$\frac{d[C]^A_{out}}{dt} = k_{f+}[C]^A_{in} - (k_{f-} + k_-)[C]^A_{out} + k_+[C]^D_{out} \quad \text{(A3.3)}$$

$$\frac{d[C]^A_{in}}{dt} = -k_{f+}[C]^A_{in} + k_{f-}[C]^A_{out} \quad \text{(A3.4)}$$

$$k_+ = \left(\frac{k^A_{m+}S^A}{k^D_{m+}S^D + k^A_{m+}S^A}\right)k^D_{m-} \quad \text{(A3.5)}$$

$$k_- = \left(\frac{k^D_{m+}S^D}{k^D_{m+}S^D + k^A_{m+}S^A}\right)k^A_{m-} \quad \text{(A3.6)}$$

FIGURE 6: Simplified kinetics for coupled spontaneous transfer and transbilayer movement. This is an equivalent kinetic model to the one in Figure 5. The model was simplified to three step reversible reactions without introducing any additional restrictions or assumptions. The mathematical solution of this simplified model (A3) yields a simpler solution compared to that for (A2) in Figure 5.

It is obvious that a more suitable mathematical solution correlated with experimental observations is needed to study the kinetic parameters for the coupled processes of spontaneous transfer and transbilayer movement. Such an approach is outlined in this appendix. First, we will simplify the kinetic model somewhat. The schematic shown in Figure 6 and the eq A3 are equivalent to that in Figure 5 and eq A2 if we introduce $K-$ and $K+$ for K_m- and K_m+ to satisfy

eqs A3.5 and 3.6. Importantly, this does not introduce any additional restrictions on the original kinetic model. However, this results in an equivalent transformation of the kinetic process from four-steps to three-steps and from eq A2 to eq A3. This equivalent transformation results in a significant simplification of the final mathematical solution without any additional restrictions on the original model.

Summary. (1) This solution can be universally applied to the kinetic model of coupled spontaneous transfer and transbilayer movement without further restrictions and is well correlated to the experimental observations which indicate coupled spontaneous transfer and transbilayer movement of lipids are usually described by a double-exponential function. (2) This solution is relatively simple compared to previous solutions involving three- and four-exponential functions. Each variable in the equations has a clear physical meaning so that it can be directly applied to experimental analysis without introducing any further restrictions.

(3) This approach can yield more accurate kinetic parameters compared to the empirical fittings noted above, by relating the pre-exponential and superexponential variables to each other and by removing the arbitrary assignment of the slow and fast phases during the analysis.

Solving Relaxation Times

Noting that there are only three independent equations in eq A3, the reciprocal relaxation times $1/\tau_j$ should be the eigen values of determinantal equation which is derived from these equations.

$$\begin{vmatrix} k_{f+} - \frac{1}{\tau} & -k_{f-} & 0 \\ -k_{f+} & k_{f-} + k_+ - \frac{1}{\tau} & -k_- \\ k_{f+} & k_{f+} - k_+ & k_{f+} + k_{f-} + k_- - \frac{1}{\tau} \end{vmatrix} \equiv 0$$

$$\downarrow$$

$$\left(\frac{1}{\tau} - k_{f+} - k_{f-}\right)\left[\frac{1}{\tau^2} - (k_{f+} + k_{f-} + k_+ + k_-)\frac{1}{\tau} + k_{f+}(k_+ + k_-)\right] \equiv 0$$

$$\downarrow$$

$$\frac{1}{\tau_1} = k_{f+} + k_{f-} \quad \text{and} \tag{A4.1}$$

$$\frac{1}{\tau_{2,3}} = [(k_{f+} + k_{f-} + k_+ + k_-) \pm [(k_{f+} + k_{f-})^2 + (k_+ + k_-)^2 + 2(k_{f-} - k_{f+})(k_+ + k_-)]^{1/2}]/2 \tag{A4.2}$$

$$\downarrow\uparrow$$

$$\text{Also, } \frac{1}{\tau_2} + \frac{1}{\tau_3} = k_{f+} + k_{f-} + k_+ + k_- \quad \text{and} \tag{A4.3}$$

$$\frac{1}{\tau_2} \times \frac{1}{\tau_3} = k_{f+}(k_+ + k_-) \tag{A4.4}$$

Assuming that both the acceptor and donor vesicles are in an equilibrium state before they are mixed together, the relaxation amplitude corresponding to each relaxation time can be calculated as follows:

$$\text{For } \frac{1}{\tau_1} = k_{f+} + k_{f-},$$

$$(a_1)^D_{in} = (a_1)^D_{out} = (a_1)^A_{out} = (a_1)^A_{in} = 0$$

$$\text{For } \frac{1}{\tau_2} + \frac{1}{\tau_3} = k_{f+} + k_{f-} + k_+ + k_- \quad \text{and}$$

$$\frac{1}{\tau_2} \times \frac{1}{\tau_3} = (k_+ + k_-)k_{f+}$$

$$(a_2)^D_{in} = \left(\frac{\tau_2}{\tau_2 - \tau_3}\right)[C_\Delta]^D_{in} \tag{A5.1}$$

$$(a_2)^D_{out} = \left(\frac{\tau_2 - (1/k_{f+})}{\tau_2 - \tau_3}\right)[C_\Delta]^D_{out} \tag{A5.2}$$

$$(a_2)^A_{out} = \left(\frac{\tau_2 - (1/k_{f+})}{\tau_2 - \tau_3}\right)[C_\Delta]^A_{out} \tag{A5.3}$$

$$(a_2)^A_{in} = \left(\frac{\tau_2}{\tau_2 - \tau_3}\right)[C_\Delta]^A_{in} \tag{A5.4}$$

$$(a_3)^D_{in} = \left(\frac{\tau_3}{\tau_3 - \tau_2}\right)[C_\Delta]^D_{in} \tag{A6.1}$$

$$(a_3)^D_{out} = \left(\frac{\tau_3 - (1/k_{f+})}{\tau_3 - \tau_2}\right)[C_\Delta]^D{}_{out} \tag{A6.2}$$

$$(a_3)^A_{out} = \left(\frac{\tau_3 - (1/k_{f+})}{\tau_3 - \tau_2}\right)[C_\Delta]^A_{out} \tag{A6.3}$$

$$(a_3)^A_{in} = \left(\frac{\tau_3}{\tau_3 - \tau_2}\right)[C_\Delta]^A_{in} \tag{A6.4}$$

The general solution of A2 or A3 could be predicted as follows:

$$[C]^D_{in} = [C_E]^D_{in} + \sum_{j=1}^{3}(a_j)^D_{in} \exp(-t/\tau_j) \tag{A7.1}$$

$$[C]^D_{out} = [C_E]^D_{out} + \sum_{j=1}^{3}(a_j)^D_{out} \exp(-t/\tau_j) \tag{A7.2}$$

$$[C]^A_{out} = [C_E]^A_{out} + \sum_{j=1}^{3}(a_j)^A_{out} \exp(-t/\tau_j) \tag{A7.3}$$

$$[C]^A_{in} = [C_E]^A_{in} + \sum_{j=1}^{3}(a_j)^A_{in} \exp(-t/\tau_j) \tag{A7.4}$$

where $[C_E]$ represents equilibrium concentrations, τ_j represents relaxation times, and a_j represents relaxation amplitudes.

Solving Equilibrium Concentrations

At $t = 0$, concentrations of donor and acceptor vesicles are $[C]_o^D$ and $[C]_o^A$, repsectively. Then,

$$[C_o]_{in}^D = \left(\frac{k_{f-}}{k_{f+} + k_{f-}}\right)[C]_o^D \text{ and } [C_o]_{out}^A = \left(\frac{k_{f+}}{k_{f+} + k_{f-}}\right)[C]_o^A$$

$$[C_o]_{out}^D = \left(\frac{k_{f+}}{k_{f+} + k_{f-}}\right)[C]_o^D \text{ and } [C_o]_{in}^A = \left(\frac{k_{f-}}{k_{f+} + k_{f-}}\right)[C]_o^A$$

At equilibrium, the following equations apply:

$$[C_E]_{in}^D = \left(\frac{k_{f-}}{k_{f+} + k_{f-}}\right)\left(\frac{k_-}{k_+ + k_-}\right)([C]_o^D + [C]_o^A) \quad \text{(A8.1)}$$

$$[C_E]_{out}^D = \left(\frac{k_{f+}}{k_{f+} + k_{f-}}\right)\left(\frac{k_-}{k_+ + k_-}\right)([C]_o^D + [C]_o^A) \quad \text{(A8.2)}$$

$$[C_E]_{in}^A = \left(\frac{k_{f-}}{k_{f-} + k_{f+}}\right)\left(\frac{k_+}{k_+ + k_-}\right)([C]_o^D + [C]_o^A) \quad \text{(A8.3)}$$

$$[C_E]_{out}^A = \left(\frac{k_{f+}}{k_{f+} + k_{f-}}\right)\left(\frac{k_+}{k_+ + k_-}\right)([C]_o^D + [C]_o^A) \quad \text{(A8.4)}$$

For change of concentrations, the following equations apply:

$$[C_\Delta]_{in}^D = \left(\frac{k_{f-}}{k_{f+} + k_{f-}}\right)\left(\frac{k_+[C]_o^D - k_-[C]_o^A}{k_+ + k_-}\right) \quad \text{(A9.1)}$$

$$[C_\Delta]_{out}^D = \left(\frac{k_{f+}}{k_{f+} + k_{f-}}\right)\left(\frac{k_+[C]_o^D - k_-[C]_o^A}{k_+ + k_-}\right) \quad \text{(A9.2)}$$

$$[C_\Delta]_{in}^A = \left(\frac{k_{f-}}{k_{f+} + k_{f-}}\right)\left(\frac{k_-[C]_o^A - k_+[C]_o^D}{k_+ + k_-}\right) \quad \text{(A9.3)}$$

$$[C_\Delta]_{out}^A = \left(\frac{k_{f+}}{k_{f+} + k_{f-}}\right)\left(\frac{k_-[C]_o^A - k_+[C]_o^D}{k_+ + k_-}\right) \quad \text{(A9.4)}$$

The following is the complete solution for eqs A2 or A3:

$$[C]_{in}^D = [C_E]_{in}^D + [C_\Delta]_{in}^D\left\{\left(\frac{\tau_2}{\tau_2 - \tau_3}\right)e^{-t/\tau_2} + \left(\frac{\tau_3}{\tau_3 - \tau_2}\right)e^{-t/\tau_3}\right\} \quad \text{(A10.1)}$$

$$[C]_{out}^D = [C_E]_{out}^D + [C_\Delta]_{out}^D\left\{\left(\frac{\tau_2 - (1/k_{f+})}{\tau_2 - \tau_3}\right)e^{-t/\tau_2} + \left(\frac{\tau_3 - (1/k_{f+})}{\tau_3 - \tau_2}\right)e^{-t/\tau_3}\right\} \quad \text{(A10.2)}$$

$$[C]_{out}^A = [C_E]_{out}^A + [C_\Delta]_{out}^A\left\{\left(\frac{\tau_2 - (1/k_{f+})}{\tau_2 - \tau_3}\right)e^{-t/\tau_2} + \left(\frac{\tau_3 - (1/k_{f+})}{\tau_3 - \tau_2}\right)e^{-t/\tau_3}\right\} \quad \text{(A10.3)}$$

$$[C]_{in}^A = [C_E]_{in}^A + [C_\Delta]_{in}^A\left\{\left(\frac{\tau_2}{\tau_2 - \tau_3}\right)e^{-t/\tau_2} + \left(\frac{\tau_3}{\tau_3 - \tau_2}\right)e^{-t/\tau_3}\right\} \quad \text{(A10.4)}$$

where $[C]_y^x$ is the lipid concentration for each compartment at time t, $[C_E]_y^x$ is the equilibrium lipid concentration for each compartment, $[C_\Delta]_y^x$ is the total change of lipid concentration for each compartment ($[C_\Delta] = [C_o] - [C_E]$), and τ_i are the relaxation times.

For special cases, (1) when $k_m^- \gg k_f$, the coupling of spontaneous transfer and flip−flop becomes weaker, we have

$$\frac{1}{\tau_2} = k_+ + k_- \quad \text{(A11.1)}$$

$$\frac{1}{\tau_3} = k_{f-} + k_{f+} \quad \text{(A11.2)}$$

Under these conditions, the kinetic process could be described as one fast phase and one slow phase. This is the theoretical basis for refs 34, 36, 38−42, which arbitrary assigned the fast phase → spontaneous transfer and the slow phase → flip−flop. (2) When k_{f+} and $k_{f-} \to 0$, we have

$$\frac{1}{\tau_2} = k_+ + k_- \quad \text{(A12.1)}$$

$$\frac{1}{\tau_3} \to 0 \quad \text{(A12.2)}$$

the kinetic process became a single exponential, which simplified to (*4*, *5*),

$$[C]_{in}^D = [C_o]_{in}^D = [C_E]_{in}^D = \frac{[C]_o^D}{2} \quad \text{(A13.1)}$$

$$[C]_{out}^D = [C_o]_{out}^D + [C_\Delta]_{out}^D e^{-t/\tau_2} \quad \text{(A13.2)}$$

$$[C]_{out}^A = [C_o]_{out}^A + [C_\Delta]_{out}^A e^{-t/\tau_2} \quad \text{(A13.3)}$$

$$[C]_{in}^A = [C_o]_{in}^A = [C_E]_{in}^A = \frac{[C]_o^A}{2} \quad \text{(A13.4)}$$

$$[C_o]_{out}^D = \frac{[C]_o^D}{2}, [C_o]_{out}^A = \frac{[C]_o^A}{2},$$

$$[C_E]_{out}^D = \left(\frac{k_-}{k_+ + k_-}\right)\left(\frac{[C]_o^A + [C]_o^D}{2}\right),$$

$$[C_E]_{out}^A = \left(\frac{k_+}{k_+ + k_-}\right)\left(\frac{[C]_o^A + [C]_o^D}{2}\right)$$

$$[C_\Delta]_{out}^D = \frac{k_+[C]_o^D - k_-[C]_o^A}{2(k_+ + k_-)},$$

$$[C_\Delta]_{out}^A = \left(\frac{k_-[C]_o^A - k_+[C]_o^D}{2(k_+ + k_-)}\right)$$

$$\frac{1}{\tau_2} = k_+ + k_- = \frac{(k^A_{m+}\, k^D_{m-})S^A + (k^D_{m+}\, k^A_{m-})S^D}{k^D_{m+}S^D + k^A_{m+}S^A}$$

which is same as the result in ref 4.

APPENDIX B: SIMPLIFICATIONS APPLIED TO THIS PAPER

(1) *Concentration Equations (A10)*: The general format of the concentration equations does not change. However, $[C_o]$, $[C_E]$, and $\tau_{2,3}$ could be simplified as follows. (1) Since LUV were used for all the measurements we have, $k_{f+} = k_{f-} = k_f$. (2) Donor and acceptor vesicles are composed of the same phospholipid (POPC). Only the donor vesicle contains small amounts of fluorescent lipid. So, $k^A_{m+} = k^D_{m+}$ and $k^A_{m-} = k^D_{m-}$. (3) The ratio of acceptor to donor vesicles was N. We have $S^A = NS^D$. So,

$$\begin{cases} k_+ = \dfrac{N}{N+1}k^-_m \\ k_- = \dfrac{1}{N+1}k^-_m \end{cases} \Leftrightarrow \begin{cases} k_+ + k_- = k_{m-} \\ \dfrac{k_+}{k_-} = N \end{cases}$$

Then, eq A4 relaxation time could be simplified to

$$\frac{1}{\tau_{2,3}} = \frac{(2k_f + k_{m-}) \pm \sqrt{4k_f^2 + k_{m-}^2}}{2} \qquad \text{(B1)}$$

The lipid concentrations of each compartment can also be simplified to

$$[C_o]^D_{in} = [C_o]^D_{out} = \frac{1}{2}[C_o],\ [C_o]^A_{in} = [C_o]^A_{out} = 0 \qquad \text{(B2.1)}$$

$$[C_E]^D_{in} = [C_E]^D_{out} = \frac{[C]^D_o}{2(N+1)},\ [C_E]^A_{in} = [C_E]^A_{out} = \frac{N[C]^D_o}{2(N+1)} \qquad \text{(B2.2)}$$

$$[C_\Delta]^D_{in} = [C_\Delta]^D_{out} = \frac{N[C]^D_o}{2(N+1)},\ [C_\Delta]^A_{in} = [C]^A_{out} = -\frac{N[C]^D_o}{2(N+1)} \qquad \text{(B2.3)}$$

(2) Ratio of Concentrations of Fluorescent Lipids vs POPC in Each Compartment.

$$[C_o\%]^D_{in} = [C_o\%]^D_{out} = \frac{C^D_o}{[POPC]^D} = [C]^D_o\%;$$
$$[C_o\%]^A_{in} = [C_o\%]^A_{out} = 0$$

$$[C_E\%]^D_{in} = [C_E\%]^D_{out} = [C_E\%]^A_{in} = [C_E\%]^A_{out} = \frac{[C]^D_o\%}{N+1}$$

$$[C_\Delta\%]^D_{in} = [C_\Delta\%]^D_{out} = \frac{N[C]^D_o\%}{N+1},$$
$$[C_\Delta\%]^A_{in} = [C_\Delta\%]^A_{out} = \frac{-[C]^D_o\%}{N+1}$$

From A10, the lipid concentrations can be converted to ratio concentrations as follows:

$$[C\%]^D_{in} = [C_E\%]^D_{in} + [C_\Delta\%]^D_{in}\left\{\left(\frac{\tau_2}{\tau_2 - \tau_3}\right)e^{-t/\tau_2} + \left(\frac{\tau_3}{\tau_3 - \tau_2}\right)e^{-t/\tau_3}\right\} \qquad \text{(B3.1)}$$

$$[C\%]^D_{out} = [C_E\%]^D_{out} + [C_\Delta\%]^D_{out}\left\{\left(\frac{\tau_2 - (1/k_f)}{\tau_2 - \tau_3}\right)e^{-t/\tau_2} + \left(\frac{\tau_3 - (1/k_f)}{\tau_3 - \tau_2}\right)e^{-t/\tau_3}\right\} \qquad \text{(B3.2)}$$

$$[C\%]^A_{out} = [C_E\%]^A_{out} + [C_\Delta\%]^A_{out}\left\{\left(\frac{\tau_2 - (1/k_f)}{\tau_2 - \tau_3}\right)e^{-t/\tau_2} + \left(\frac{\tau_3 - (1/k_f)}{\tau_3 - \tau_2}\right)e^{-t/\tau_3}\right\} \qquad \text{(B3.3)}$$

$$[C\%]^A_{in} = [C_E\%]^A_{in} + [C_\Delta\%]^A_{in}\left\{\left(\frac{\tau_2}{\tau_2 - \tau_3}\right)e^{-t/\tau_2} + \left(\frac{\tau_3}{\tau_3 - \tau_2}\right)e^{-t/\tau_3}\right\} \qquad \text{(B3.4)}$$

(3) Fluorescence Intensity.
At time t, $F(t) = F(t)^D_{in} + F(t)^D_{out} + F(t)^A_{out} + F(t)^A_{in}$.

$$\text{Also,}\quad F(t) = SC([C\%]^D_{in}) + SC([C\%]^D_{out}) + N\{SC([C\%]^A_{out}) + SC([C\%]^A_{in})\} \qquad \text{(B4)}$$

A short program containing the above equation was compiled in Fortran 77 and linked to the NONLIN fitting program.

(4) Estimation of Kinetic Constants before Calculations.

$$F(t) = SC([C\%]^D_{in}) + SC([C\%]^D_{out}) + NSC([C\%]^A_{in}) + NSC([C\%]^A_{out})$$

$$\frac{dF}{dt} = \left.\frac{dSC}{dC}\right|_{C=[C\%]^D_{in}}\frac{d[C\%]^D_{in}}{dt} + \left.\frac{dSC}{dC}\right|_{C=[C\%]^D_{out}}\frac{d[C\%]^D_{out}}{dt} + N\left.\frac{dSC}{dC}\right|_{C=[C\%]^A_{out}}\frac{d[C\%]^A_{out}}{dt} + N\left.\frac{dSC}{dC}\right|_{C=[C\%]^A_{in}}\frac{d[C\%]^A_{in}}{dt}$$

Also, $[C\%] = (C/C_{POPC}) \times 100\%$, therefore,

$$\frac{dF}{dt} = \frac{2}{[C_{POPC}]^D}\left\{\left.\frac{dSC}{dC}\right|_{[C\%]^D_{in}}\frac{d[C]^D_{in}}{dt} + \left.\frac{dSC}{dC}\right|_{[C\%]^D_{out}}\frac{d[C]^D_{out}}{dt} + \left.\frac{dSC}{dC}\right|_{[C\%]^A_{out}}\frac{d[C]^A_{out}}{dt} + \left.\frac{dSC}{dC}\right|_{[C\%]^A_{in}}\frac{d[C]^A_{in}}{dt}\right\} = \left\{k_f([C]^D_{in} - [C]^D_{out})\left(\left.\frac{dSC}{dC}\right|_{[C\%]^D_{out}} - \left.\frac{dSC}{dC}\right|_{[C\%]^D_{in}}\right) + (k_+[C\%]^D_{out} - k_-[C]^A_{out})\left(\left.\frac{dSC}{dC}\right|_{[C\%]^A_{out}} - \left.\frac{dSC}{dC}\right|_{[C\%]^D_{out}}\right) + k_f([C]^A_{in} - [C]^A_{out})\left(\left.\frac{dSC}{dC}\right|_{[C\%]^A_{out}} - \left.\frac{dSC}{dC}\right|_{[C\%]^A_{in}}\right)\right\}\frac{2}{[C_{POPC}]^D}$$

When $t = 0$, $[C_o]^D_{in} = [C_o]^D_{out} = [C_o]/2$, and $[C]^A_{in} = [C]^A_{out} = 0$:

$$\left.\frac{dF}{dt}\right|_{t=0} = \frac{2}{[C_{POPC}]^D}(k_+[C]^D_{out} - k_-[C]^A_{out})\left(\left.\frac{dSC}{dC}\right|_{[C\%]^A_{out}} - \left.\frac{dSC}{dC}\right|_{[C\%]^D_{out}}\right)\Bigg|_{t=0} = \frac{2}{[C_{POPC}]^D}k_+[C_o]^D_{out}\left(\left.\frac{dSC}{dC}\right|_{0\%} - \left.\frac{dSC}{dC}\right|_{10\%}\right) = 10\%k_+\left(\left.\frac{dSC}{dC}\right|_{0\%} - \left.\frac{dSC}{dC}\right|_{10\%}\right)$$

$$k_+ = 10 \times \left.\frac{dF}{dt}\right|_{t=0} \Big/ \left(\left.\frac{dSC}{dC}\right|_{0\%} - \left.\frac{dSC}{dC}\right|_{10\%}\right) \quad \text{(B5.1)}$$

$$k_- = \frac{k_+}{N} \quad \text{(B5.2)}$$

$$k_{m-} = k_+ + k_- \quad \text{(B5.3)}$$

The kinetic parameters for spontaneous transfer could be estimated from the initial increase in rate of fluorescence intensity.

REFERENCES

1. Pagano, R. E., and Sleight, R. G. (1975) *Science 229*, 1051−1057.
2. Hoekstra, D., and Kok, J. W. (1992) *Biochim. Biophys. Acta 1113*, 277−294.
3. Rosenwald, A. G., and Pagano, R. E. (1993) *Adv. Lipid Res. 26*, 101−118.
4. Nichols, J. W., and Pagano, R. E. (1981) *Biochemistry 20*, 2783−2789.
5. Nichols, J. W., and Pagano, R. E. (1982) *Biochemistry 21*, 1720−1726.
6. Pagano, R. E., and Longmuir, K. J. (1985) *J. Biol. Chem. 260*, 1909−1916
7. Pagano, R. E., and Martin, O. C. (1988) *Biochemistry 27*, 4439−4445.
8. Pagano, R. E. *(1989) Methods in Cell Biology: Fluorescence Microscopy of Living Cell in Culture*, Vol. 29, Chapter 5, Academic Press, Inc., San Diego.
9. Martin, O. C., and Pagano, R. E. (1987) *J. Biol. Chem. 262*, 5890−5898.
10. Sleight, R. G., and Abanto, M. N. (1989) *J. Cell Sci. 93*, 363−374.
11. Connor, J., Pak, C. H., Zwall, R. F. A., and Schroit, A. J. (1992) *J. Biol. Chem. 267*, 19412−19417.
12. Menon, A. K. (1995) *Trends Cell Biol. 5*, 355−360.
13. Kean, L. S., Fuller, R. S., and Nichols, J. W. (1993) *J. Cell Biol. 123*, 1403−1419.
14. Pagano, R. E., Martin, O. C., Kang, H. C., and Haugland, R. P. (1991) *J. Cell Biol. 113*, 1267−1279.
15. (a) Martin, O. C., and Pagano, R. E. (1994) *J. Cell Biol. 125*, 769−781. (b) Chen, C. S., Martin, O. C., and Pagano, R. E. (1997) *Biophys. J. 72*, 37−50.
16. Johnson, I. D., Kang, H. C., and Haugland, R. P. (1991) *Anal. Biochem. 198*, 228−237.
17. Chattopadhyay, A., and London, E. (1987) *Biochemistry 26*, 39−45.
18. Wolf, D. E., Winiski, A. P., Ting, A. E., Bocian, K. M., and Pagano, R. E. (1992) *Biochemistry 31*, 2865−2873.
19. Nakagawa, T. (1974) *Colloid Polym. Sci. 252*, 56−64.
20. Thilo, L. (1977) *Biochim. Biophys. Acta 469*, 326−334.
21. Nichols, J. W. and Pagano, R. E. (1981) *Biochemistry 20*, 2783−2789.
22. Nichols, J. W., and Pagano, R. E. (1982) *Biochemistry 21*, 1720−2726.
23. Kates, M. (1972) in *Techniques of Lipidology* (Work, T. S., and Work, E., Eds.) Elsevier Scientific Publishing Co., Amsterdam.
24. Rouser, B., Siakotos, A. N., and Fleisher, S. (1981) *Lipids 1*, 85−86.
25. Hope, M. J., Bally, M. B., Webb, G., and Cullis, P. R. (1985) *Biochim. Biophys. Acta 812*, 55−65.
26. (a) Brown, M. P., Shaikh, N., Brenowitz, M., and Brand, L (1994) *J. Biol. Chem. 269*, 12600−12605. (b) Johnson, M. L., and Faunt, L. M. (1992) *Methods Enzymol. 210*, 1−37.
27. Struck, D. K., and Pagano, R. E. (1980) *J. Biol. Chem. 255*, 5405−5410.
28. van Meer, G., Stelzer, E. H. K., Wijnaendts-van-Resandt, R. W., and Simons, K. (1987) *J. Cell Biol. 105*, 1623−1635.
29. Brown, R. E. (1992) *Biochim. Biophys. Acta 1113*, 375−389.
30. Thompson, T. E. (1978) in *Molecular Specialization and Symmetry in Membrane Function*, pp 18−98, Harvard University Press, Cambridge, MA.
31. Quinn, P. J. (1981) *Prog. Biophys. Mol. Biol. 38*, 1.
32. Dekruijtt, B., and van Zoellen, E. J. J. (1978) *Biochim. Biophys. Acta 551*, 105−115.
33. McLean, L. R., and Phillips, M. C. (1984) *Biochemistry 23*, 4624−4630.
34. Wimley, W. C., and Thompson, T. E. (1990) *Biochemistry 29*, 1295−1303.
35. Voet, D., and Voet, J. (1990) *Biochemistry*, p 1158, John Wiley & Sons, New York.
36. Arvinte, T., and Hildenbrand, K. (1984) *Biochim. Biophys. Acta 775*, 86−94.
37. Storch, J., and Kleinfied, A. M. (1986) *Biochemistry 25*, 1717−1726.
38. De Kruijff, B., and Van Zoellen, E. J. J. (1978) *Biochim. Biophys. Acta 511*, 105−115.
39. Mclean, L. R., and Phillips, M. C. (1984) *Biochemistry 23*, 4624−4630.
40. Bayerl, T. M., Schmidt, C., and Sackmann, E. (1988) *Biochemistry 27*, 6078−6085.
41. Homan, R., and Pownall, H. J. (1988) *Biochim. Biophys. Acta 938*, 155−166.
42. William, C. W., and Thompson, T. E. (1991) *Biochemistry 30*, 1702−1709.

BI970145R